Fermionic dark matter in radiative inverse seesaw model with U(1) B-L

doi: 10.1103/PhysRevD.86.033011

KANAZAWA-12-05, P12039

Fermionic Dark Matter in Radiative Inverse Seesaw Model with $U(1)_{B-L}$

Hiroshi Okada,[a1] Takashi Toma[b2]

[a] *School of Physics, KIAS, Seoul 130-722, Korea*

[b] *Institute for Theoretical Physics, Kanazawa University, Kanazawa, 920-1192, Japan*

Abstract

We construct a radiative inverse seesaw model with local $B-L$ symmetry, and investigate the flavor structure of the lepton sector and the fermionic Dark Matter. Neutrino masses are radiatively generated through a kind of inverse seesaw framework. The PMNS matrix is derived from each mixing matrix of the neutrino and charged lepton sector with large Dirac CP phase. We show that the annihilation processes via the interactions with Higgses which are independent on the lepton flavor violation, have to be dominant in order to satisfy the observed relic abundance by WMAP. The new interactions with Higgses allow us to be consistent with the direct detection result reported by XENON100, and it is possible to verify the model by the exposure of XENON100 (2012).

[1] HOkada@kias.re.kr

[2] t-toma@hep.s.kanazawa-u.ac.jp

1 Introduction

Inverse seesaw mechanism which generates neutrino masses due to small lepton number violation is one of the intriguing way to describe tiny neutrino masses [1, 2]. Thus interesting phenomenological implications have been accommodated [3–5]. However Dark Matter (DM) candidate has to be introduced independently if we discuss DM phenomenology in this kind of models. On the other hand, radiative seesaw mechanism is possible to relate neutrino mass generation with the existence of DM [6–8]. In particular, the radiative seesaw model which is proposed by Ma [6] is the simplest model with DM candidates. Subsequently there are a lot of recent works of the model [9–11] and the extended models [12–19]. The other radiative neutrino mass models are studied in Refs. [20–23]. The $\mathbb{Z}_2$ parity imposed to the model forbids to have the Dirac neutrino masses, produces neutrino masses at one loop level, and stabilizes DM candidates. Therefore the feature of the radiative seesaw model motivates to connect the existence of DM with the neutrino mass generation due to inverse seesaw mechanism.

In this paper, we construct a radiative inverse seesaw model with $U(1)_{B-L}$ as a concrete example and analyze the neutrino masses, mixing and the feature of DM. We add three pairs of $B-L$ charged fermions and a scalar to Ma model [6]. The scalar particle breaks the $B-L$ symmetry spontaneously. In the model, the small Majorana mass terms which violate $U(1)_{B-L}$ weakly and explain the tiny neutrino masses are generated from a higher operator when the $U(1)_{B-L}$ symmetry is spontaneously broken. We assume the structure of neutrino mass matrix that induces the best fit value of θ_{12} of the Pontecorvo-Maki-Nakagawa-Sakata (PMNS) neutrino mixing matrix [24]: $\sin^2\theta_{12}$=0.311, which is within 1σ confidence level in the global analysis [25]. Moreover, we introduce the charged-lepton mixing (λ) with nonzero Dirac CP phase to induce non-zero θ_{13} recently reported by T2K [26], Double Chooz [27], Daya-Bay [28], and RENO [29]. This method was firstly proposed by S. King [30, 31]. Due to the mixing λ, neutrino Dirac Yukawa couplings are strongly constrained by the lepton flavor violation (LFV), especially, $\mu \to e\gamma$ process. Hence in the original radiative seesaw model [6], it is hard to derive the observed relic density of DM [32] associated to the annihilation channel if we assume that the lightest right-handed neutrino is DM. However since the radiative inverse seesaw model has the other channels with different coupling due to the additional Higgs boson coming from the $B-L$ symmetry, the observed relic abundance can be naturally obtained via the channel. Since the additional Higgs boson mixes with the SM like Higgs, the direct detection with Higgs portal also comes into the target of a discussion whether the result can be consistent with the experimental limit reported by XENON100 [33]. It implies that the model can be investigated in the direct search of

DM near future. Therefore it is favored to be Higgs portal DM in the radiative inverse seesaw model from the consistency with neutrino masses, mixing, LFV and the DM property.

This paper is organized as follows. In Section 2, we construct the radiative inverse seesaw model and its Higgs sector. In Section 3, we discuss the constraints from LFV, especially, $\mu \to e\gamma$ process and the DM relic abundance. In Section 4, we analyze the direct detection of our DM including all the other constraint. We summarize and conclude the paper in Section 5.

2 The Radiative Inverse Seesaw Model

2.1 Neutrino Mass and Mixing

Particle	Q	u^c, d^c	L	e^c	N^c	S	S'	Φ	η	χ
$SU(2)_L$	**2**	**1**	**2**	**1**	**1**	**1**	**1**	**2**	**2**	**1**
Y_{B-L}	1/3	-1/3	-1	1	1	-1/2	1/2	0	0	-1/2
$\mathbb{Z}_2$	+	+	+	+	−	−	+	+	−	+

Table 1: The field contents and the charges. Three generations of right handed neutrinos N_i^c and additional fermions S_i, S_i' are introduced. A pair of fermions S and S' is required to cancel the anomaly. The SM, inert and $B-L$ Higgs bosons are denoted by Φ, η, and χ, respectively.

The radiative inverse seesaw mechanism can be realized by introducing the $B-L$ symmetry which is spontaneously broken at TeV scale [4]. The field contents of our model is shown in Table 1 and the Lagrangian in the lepton sector is

$$\mathcal{L} = y_\ell L\Phi e^c + y_\nu L\eta N^c + y_S N^c \chi S + \frac{\lambda_S}{\Lambda}\chi^{\dagger 2} S^2 + \frac{\lambda_{S'}}{\Lambda}\chi^2 S'^2 + \text{h.c.}, \tag{2.1}$$

where Λ is a cut-off scale and the generation indices are abbreviated. Note that the mass term SS' can be forbidden by the Z_2 symmetry[1]. We have another dimension 5 operator such as $L\Phi S'\chi^\dagger$, which affects on the neutrino mass, and it would be difficult to forbid it. Thus we need to assume the coupling of this operator is small enough.

After the symmetry breaking, that is $\chi = (\chi^0 + v')/\sqrt{2}$ [2], $\phi = (\phi^0 + v)/\sqrt{2}$ with $\Phi = (\phi^+, \phi)^T$

[1] Another way to induce the mass term of S is proposed by E. Ma [34], in which the term is done at loop level.

[2] The value of v' can be constrained by the LEP experiment that tells us $m_{Z'}/g' = |Y^\chi_{B-L}|v' > 6$ TeV [35], where $m_{Z'}$ and g' are the $B-L$ gauge boson and the $B-L$ guage coupling, respectively. Since Y^χ_{B-L}=-1/2 is taken in our case, $v' > 12$ TeV is obtained.

and $v = 246$ GeV, the neutrino sector in the flavor basis can be written as

$$\mathcal{L}_m^\nu = y_\nu L\eta N^c + M^T N^c S + \frac{\mu}{2} S^2 + \text{h.c.}, \tag{2.2}$$

where $M = y_S v'/\sqrt{2}$ and $\mu = \lambda_S v'^2/\Lambda$. The scale of $\mu \sim 1$ keV which corresponds to $\Lambda \sim 10^{14}$ GeV is required as we will see in the following section. The inert doublet $\eta \equiv (\eta^+, (\eta_R + i\eta_I)/\sqrt{2})^T$ does not have any vacuum expectation values (VEV). As a result, the 6×6 neutrino mass matrix in the basis (N^c, S) takes the form:

$$\mathcal{M}_\nu = \begin{pmatrix} 0 & M^T \\ M & \mu \end{pmatrix}. \tag{2.3}$$

The mass matrix M and μ cannot be diagonalized simultaneously in general. We assume that the mass matrix M and μ are diagonal as $M = \text{diag}\,(M_1, M_2, M_3)$ and $\mu = \text{diag}\,(\mu_1, \mu_2, \mu_3)$ for simplicity. Then the 6×6 mass matrix $\mathcal{M}_\nu$ can be diagonalized for every family as $\text{diag}(m_{i+}, m_{i-})$ by the unitary matrix U_i for i-th family. The mass eigenvalues are expressed as

$$m_{i\pm} = \sqrt{M_i^2 + \frac{\mu_i^2}{4}} \pm \frac{\mu_i}{2}. \tag{2.4}$$

When $\mu_i \ll M_i$, the neutrino masses are degenerated. The unitary matrix U_i can be expressed as

$$U_i = \begin{pmatrix} \frac{M_i}{\sqrt{M_i^2+m_{i+}^2}} & \frac{iM_i}{\sqrt{M_i^2+m_{i-}^2}} \\ \frac{m_{i+}}{\sqrt{M_i^2+m_{i+}^2}} & -\frac{im_{i-}}{\sqrt{M_i^2+m_{i-}^2}} \end{pmatrix}, \tag{2.5}$$

where $(m_{i+}, m_{i-}) = U_i^T \mathcal{M}_\nu^i U_i$ and $\mathcal{M}_\nu^i$ implies the 2×2 mass matrix for i-th family. The flavor eigenstates are rewritten by the mass eigenstates $\nu_{i\pm}$ as follows:

$$N_i^c = \frac{M_i}{\sqrt{M_i^2 + m_{i+}^2}}\nu_{i+} + \frac{iM_i}{\sqrt{M_i^2 + m_{i-}^2}}\nu_{i-}, \tag{2.6}$$

$$S_i = \frac{m_{i+}}{\sqrt{M_i^2 + m_{i+}^2}}\nu_{i+} - \frac{im_{i-}}{\sqrt{M_i^2 + m_{i-}^2}}\nu_{i-}. \tag{2.7}$$

The light neutrino mass matrix seen in Fig. 1 is given as Ref. [6] by 1-loop radiative correction:

$$\begin{aligned}(m_\nu)_{\alpha\beta} = &-\sum_{i=1}^{3} \frac{(y_\nu)_{\alpha i}(y_\nu)_{\beta i}}{(4\pi)^2} \frac{M_i^2 m_{i-}}{M_i^2 + m_{i-}^2} \left[\frac{m_R^2}{m_R^2 - m_{i-}^2} \log \frac{m_R^2}{m_{i-}^2} - \frac{m_I^2}{m_I^2 - m_{i-}^2} \log \frac{m_I^2}{m_{i-}^2} \right] \\ &+ \sum_{i=1}^{3} \frac{(y_\nu)_{\alpha i}(y_\nu)_{\beta i}}{(4\pi)^2} \frac{M_i^2 m_{i+}}{M^2 + m_{i+}^2} \left[\frac{m_R^2}{m_R^2 - m_{i+}^2} \log \frac{m_R^2}{m_{i+}^2} - \frac{m_I^2}{m_I^2 - m_{i+}^2} \log \frac{m_I^2}{m_{i+}^2} \right], \end{aligned} \tag{2.8}$$

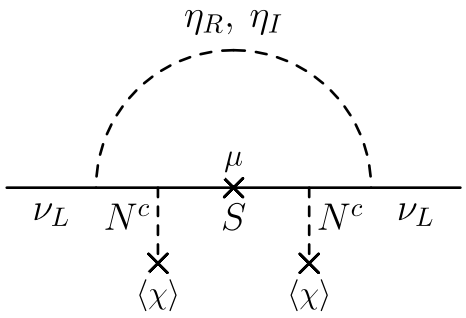

Figure 1: Neutrino mass generation via radiative inverse seesaw.

where m_R and m_I imply masses of η_R and η_I. When $\mu_i \ll M_i$, we can obtain the approximate light neutrino mass matrix by expanding $m_{i\pm}$ up to the leading order,

$$(m_\nu)_{\alpha\beta} \simeq -\sum_{i=1}^{3} \frac{(y_\nu)_{\alpha i}\,(y_\nu)_{\beta i}\,\mu_i}{2(4\pi)^2}\left[\frac{m_R^2}{M_i^2} I\left(\frac{M_i^2}{m_R^2}\right) - \frac{m_I^2}{M_i^2} I\left(\frac{M_i^2}{m_I^2}\right)\right] + \mathcal{O}\left(\mu_i^2\right), \tag{2.9}$$

where we will define the function $I(x)$ and the parameter Λ_i as

$$I(x) = \frac{x}{1-x}\left(1 + \frac{x\log x}{1-x}\right),\ \Lambda_i = \frac{\mu_i}{2(4\pi)^2}\left[\frac{m_R^2}{M_i^2} I\left(\frac{M_i^2}{m_R^2}\right) - \frac{m_I^2}{M_i^2} I\left(\frac{M_i^2}{m_I^2}\right)\right]. \tag{2.10}$$

We can see from Eq. (2.9) that the mixing matrix of the light neutrino mass matrix is determined by the structure of the neutrino Yukawa matrix y_ν since the majorana mass matrix μ is assumed to be diagonal in this case. In order to identify the structure of y_ν, here we set a specific texture of the neutrino mass matrix, which induces the best fit values of θ_{12}, as

$$m_\nu = \begin{pmatrix} A & B & -B \\ B & (3A+\sqrt{3}B)/6 & -(3A+\sqrt{3}B)/6 \\ -B & -(3A+\sqrt{3}B)/6 & (3A+\sqrt{3}B)/6 \end{pmatrix}. \tag{2.11}$$

Then the mass matrix can be diagonalized by the following mixing matrix and the eigenvalues are written as

$$O_{\nu L} = \begin{pmatrix} \sqrt{(1+1/\sqrt{7})/2} & -\sqrt{(1-1/\sqrt{7})/2} & 0 \\ -\sqrt{1-1/\sqrt{7}}/2 & -\sqrt{1+1/\sqrt{7}}/2 & 1/\sqrt{2} \\ \sqrt{1-1/\sqrt{7}}/2 & \sqrt{1+1/\sqrt{7}}/2 & 1/\sqrt{2} \end{pmatrix}, \tag{2.12}$$

$$m_1 = A + \frac{2B}{\sqrt{3}}\left(1-\sqrt{7}\right),\ m_2 = A + \frac{B}{\sqrt{3}}\left(1+\sqrt{7}\right),\ m_3 = 0. \tag{2.13}$$

Thus the squared mass differences are $\Delta m^2_{\mathbf{sol}} \equiv m_2^2 - m_1^2$ and $\Delta m^2_{\mathbf{atm}} \equiv |m_1^2 - m_3^2|$, and the neutrino mass hierarchy is predicted to be inverted. In order to get $\Delta m^2_{\mathbf{sol}} = 7.62 \times 10^{-5}$ eV^2, $\Delta m^2_{\mathbf{atm}} = 2.40 \times 10^{-3}$ eV^2, which are the best fit values [25], we find the following solutions:

$$(A, B) \;=\; (\pm 4.92 \times 10^{-2},\ \pm 2.53 \times 10^{-4}), \quad (\pm 1.83 \times 10^{-2},\ \mp 3.23 \times 10^{-2})\ \text{eV}. \tag{2.14}$$

Notice that the other solutions do not exist any more. We cannot obtain non-zero $\sin\theta_{13}$ from the light neutrino mass matrix Eq. (2.11). Non-zero $\sin\theta_{13}$ is derived from the charged lepton mixing as we will discuss below. We find $\sum_i m_i \simeq 7.7 \times 10^{-4}$ eV, and the effective mass $\langle m_{ee} \rangle \equiv |\sum_i (O_{\nu L})^2_{1i} m_i| \simeq 0.026$ eV and $\tan\theta_{12} = \left(1 - \sqrt{7}\right)/\sqrt{6}$ which gives $\sin^2\theta_{12} = 0.311$ which is the best fit 1σ value [25]. The recent experimental value for $\langle m_{ee} \rangle$ are referred in Ref. [36]. We can choose the following texture which leads the above neutrino mass matrix[3] :

$$y_\nu = \begin{pmatrix} 0 & 0 & b \\ a & 0 & c \\ -a & 0 & -c \end{pmatrix}, \tag{2.15}$$

where the parameters a, b, c are expressed by A and B as follows:

$$a \;=\; \frac{1}{\sqrt{2A\Lambda_1}} \sqrt{\left(A + \frac{1+\sqrt{7}}{\sqrt{3}} B\right)\left(A + \frac{1-\sqrt{7}}{\sqrt{3}} B\right)},\ b = \frac{A}{\sqrt{A\Lambda_3}},\ c = \frac{B}{\sqrt{A\Lambda_3}}. \tag{2.16}$$

To induce non-zero θ_{13}, we consider the charged lepton mixing [30, 31]. If we set the Dirac mass matrix of charged leptons m_e and the mixing matrix U_{eL} as

$$m_e = \frac{v}{\sqrt{2}} \begin{pmatrix} y_1^\ell & y_2^\ell & 0 \\ y_2^\ell & y_3^\ell & 0 \\ 0 & 0 & y_4^\ell \end{pmatrix}, \quad U_{eL} \sim \begin{pmatrix} 1 & \lambda e^{i\delta} & 0 \\ -\lambda e^{-i\delta} & 1 & 0 \\ 0 & 0 & 1 \end{pmatrix}, \tag{2.17}$$

where we define $(|m_e|^2, |m_\mu|^2, |m_\tau|^2) = U_{eL}^\dagger m_e m_e^\dagger U_{eL}$ and δ is the Dirac CP phase. From the mixing matrix $O_{\nu L}$ and U_{eL}, we can obtain each of the element of the PMNS matrix, which is defined as $U_{PMNS} = U_{eL}^\dagger O_\nu P$, is found by

$$\sin\theta_{13} \simeq -\frac{\lambda}{\sqrt{2}},\ \sin\theta_{12} \simeq -\sqrt{(1 - 1/\sqrt{7})/2} + \frac{\lambda}{\sqrt{2}} \sqrt{(1 + 1/\sqrt{7})/2} \cos\delta,\ \sin\theta_{23} \simeq \frac{1}{\sqrt{2}}, \tag{2.18}$$

[3]Our parametrization is taken so that DM ν_{1-} couples to the charged leptons. Even if one selects another parametrization, *e.g*, by replacing the first column and the second one of y_ν, the severe constraints from LFV do not change as we will discuss in the next section.

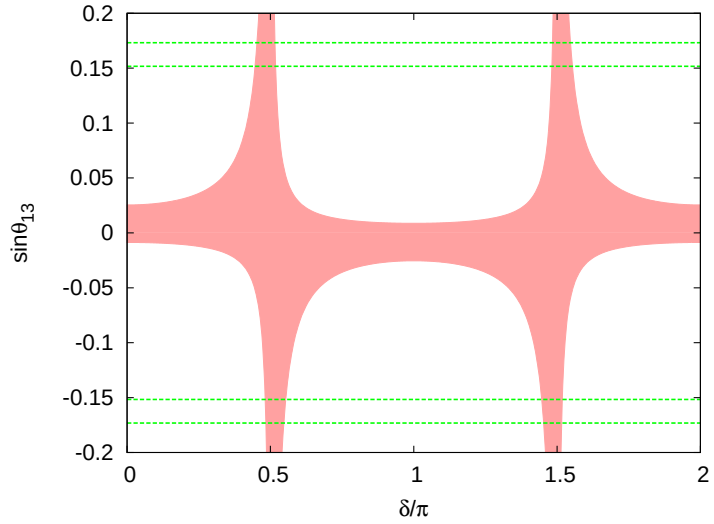

Figure 2: $\sin\theta_{13}$ versus CP Dirac phase δ. Here we restrict $\sin\theta_{12}$ within the range of the best fit with 1σ that is $0.303 \leq \sin^2\theta_{12} \leq 0.335$ [25].

where P contains two majorana phases. The allowed value of $\sin\theta_{13}$ is shown in Fig. 2 as the function of δ, within the range of the best fit with 1σ that is $0.303 \leq \sin^2\theta_{12} \leq 0.335$ [25]. The light red region is in 1σ range of $\sin\theta_{12}$. It suggests that large CP Dirac phase is required to satisfy the current global experimental limit of $\sin\theta_{13}$ for inverted hierarchy such as $0.023 \leq \sin^2\theta_{13} \leq 0.030$ [25] which is shown as the two green sandwiched regions.

2.2 Higgs Sector

The Higgses ϕ^0 and χ^0 mix after the symmetry breaking and these are not mass eigenstates. Interactions should be written by mass eigenstates in order to analyze the DM relic density and direct detection in the next section. The Higgs potential of this model is given by

$$\begin{aligned} V = {} & m_1^2\Phi^\dagger\Phi + m_2^2\eta^\dagger\eta + m_3^2\chi^\dagger\chi + \lambda_1(\Phi^\dagger\Phi)^2 + \lambda_2(\eta^\dagger\eta)^2 + \lambda_3(\Phi^\dagger\Phi)(\eta^\dagger\eta) + \lambda_4(\Phi^\dagger\eta)(\eta^\dagger\Phi) \\ & + \lambda_5[(\Phi^\dagger\eta)^2 + \text{h.c.}] + \lambda_6(\chi^\dagger\chi)^2 + \lambda_7(\chi^\dagger\chi)(\Phi^\dagger\Phi) + \lambda_8(\chi^\dagger\chi)(\eta^\dagger\eta), \end{aligned} \tag{2.19}$$

where λ_5 has been chosen real without any loss of generality. The couplings λ_1, λ_2 and λ_6 have to be positive to stabilize the potential. Inserting the tadpole conditions; $m_1^2 = -\lambda_1 v^2 - \lambda_7 v'^2/2$ and

$m_3^2 = -\lambda_6 v'^2 - \lambda_7 v^2/2$, the resulting mass matrices are given by

$$m^2(\phi^0, \chi^0) = \begin{pmatrix} 2\lambda_1 v^2 & \lambda_7 v v' \\ \lambda_7 v v' & 2\lambda_6 v'^2 \end{pmatrix} = \begin{pmatrix} \cos\alpha & \sin\alpha \\ -\sin\alpha & \cos\alpha \end{pmatrix} \begin{pmatrix} m_h^2 & 0 \\ 0 & m_H^2 \end{pmatrix} \begin{pmatrix} \cos\alpha & -\sin\alpha \\ \sin\alpha & \cos\alpha \end{pmatrix}, \tag{2.20}$$

$$m^2(\eta^\pm) = m_2^2 + \frac{1}{2}\lambda_3 v^2 + \frac{1}{2}\lambda_8 v'^2, \tag{2.21}$$

$$m_R^2 \equiv m^2(Re\eta^0) = m_2^2 + \frac{1}{2}\lambda_8 v'^2 + \frac{1}{2}(\lambda_3 + \lambda_4 + 2\lambda_5)v^2, \tag{2.22}$$

$$m_I^2 \equiv m^2(Im\eta^0) = m_2^2 + \frac{1}{2}\lambda_8 v'^2 + \frac{1}{2}(\lambda_3 + \lambda_4 - 2\lambda_5)v^2, \tag{2.23}$$

where h implies SM-like Higgs and H is an additional Higgs mass eigenstate. The tadpole condition for η, which is given by $\left.\frac{\partial V}{\partial \eta}\right|_{\rm VEV} = 0$, tells us that

$$m_2^2 > 0,\ \lambda_2 > 0,\ \lambda_3 + \lambda_4 + 2\lambda_5 > 0,\ \lambda_8 > 0, \tag{2.24}$$

in order to satisfy the condition $v_\eta = 0$ at tree level. The masses of ϕ^0 and χ^0 are rewritten in terms of the mass eigenstates of h and H as

$$\begin{aligned} \phi^0 &= h\cos\alpha + H\sin\alpha, \\ \chi^0 &= -h\sin\alpha + H\cos\alpha. \end{aligned} \tag{2.25}$$

3 The Constraints from Lepton Flavor Violation and DM Relic Density

3.1 Lepton Flavor Violation

We investigate Lepton Flavor Violation (LFV) under the flavor structure Eq. (2.15). We put a reasonable approximation $m_{i\pm} \simeq M_i$ hereafter, since the scale of μ that is keV scale is negligible compared to the scale of M_i that is expected $\mathcal{O}(10^{2\sim3})$ GeV. The experimental upper bounds of the branching ratios are $\mathrm{Br}\,(\mu \to e\gamma) \leq 2.4 \times 10^{-12}$ [37], $\mathrm{Br}\,(\tau \to \mu\gamma) \leq 4.4 \times 10^{-8}$ and $\mathrm{Br}\,(\tau \to e\gamma) \leq 3.3 \times 10^{-8}$ [38]. The branching ratios of the processes $\ell_\alpha \to \ell_\beta\gamma$ $(\ell_\alpha, \ell_\beta = e, \mu, \tau)$ are calculated as

$$\mathrm{Br}(\ell_\alpha \to \ell_\beta\gamma) = \frac{3\alpha_{\rm em}}{64\pi(G_F M_\eta^2)^2} \left| \sum_{i=1}^{3} \left(U_{eL}^\dagger y_\nu^\dagger\right)_{\alpha i} \left(y_\nu U_{eL}\right)_{i\beta} F_2\left(\frac{M_i^2}{M_\eta^2}\right) \right|^2 \mathrm{Br}(\ell_\alpha \to \ell_\beta \overline{\nu_\beta} \nu_\alpha), \tag{3.1}$$

where $\alpha_{\rm em} = 1/137$, $\mathrm{Br}\left(\mu \to e\overline{\nu_e}\nu_\mu\right) = 1.0$, $\mathrm{Br}\left(\tau \to e\overline{\nu_e}\nu_\tau\right) = 0.178$, $\mathrm{Br}\left(\tau \to \mu\overline{\nu_\mu}\nu_\tau\right) = 0.174$, M_η is η^+ mass, G_F is the Fermi constant and the loop function $F_2(x)$ is given by

$$F_2(x) = \frac{1 - 6x + 3x^2 + 2x^3 - 6x^2 \ln x}{6(1-x)^4}. \tag{3.2}$$

The $\mu \to e\gamma$ process gives the most stringent constraint. If the mixing matrix of the charged leptons Eq. (2.17) is diagonal, i.e. $\lambda = 0$, the $\mu \to e\gamma$ process does not constrain the model since the branching ratio Eq. (3.1) can be zero. Although $\tau \to \mu\gamma$ and $\tau \to e\gamma$ processes remain as LFV constraint, these are much weaker than $\mu \to e\gamma$. Instead of that, non-zero θ_{13} is not derived. Thus we can insist that $\mu \to e\gamma$ constraint is closely correlated with non-zero θ_{13}. In order to be consistent with LFV and obtaining non-zero θ_{13}, the neutrino Yukawa couplings must be small enough to escape the LFV constraint.

3.2 DM Relic Density

If we assume that DM is fermionic and mass hierarchy $M_1 < M_2 < M_3$ for the right-handed neutrinos N_i, the mass eigenstates $\nu_{1\pm}$ can be highly degenerated DMs due to the weak lepton number violation term μ_i which induces small neutrino masses. Thus we have to take into account coannihilation of ν_{1-} and ν_{1+}. The typical interacting terms are found as

$$\begin{aligned}\mathcal{L}_{\rm int} \simeq & \left(U_{eL} y_\nu\right)_{\alpha 1} \left(\overline{\ell_\alpha}\eta^+ - \overline{\nu_\alpha}\eta^0\right)\left[-\frac{i}{\sqrt{2}}\nu_{1-} + \frac{1}{\sqrt{2}}\nu_{1+}\right] + \text{h.c.} \\ & + \frac{(y_S)_{11}\sin\alpha}{2} h\left(\nu_{1-}^2 + \nu_{1+}^2\right) - \frac{(y_S)_{11}\cos\alpha}{2} H\left(\nu_{1-}^2 + \nu_{1+}^2\right) \\ & + \frac{y_f \cos\alpha}{\sqrt{2}} h\overline{f}f + \frac{y_f \sin\alpha}{\sqrt{2}} H\overline{f}f,\end{aligned} \tag{3.3}$$

where the masses of $\eta^{0(\pm)}$ assumed to be always heavier than $\nu_\pm$ to avoid the too short lifetime of DMs through our analysis. Three types of the coannihilation processes exist and these are shown in Fig 3. The effective cross section to $\ell\overline{\ell}$, $f\overline{f}$ and hh are given as

$$\sigma^\ell_{\rm eff} v_{\rm rel} \simeq \frac{1}{96\pi}\left(\sum_{\alpha=e}^{\tau} \left|\left(U_{eL} y_\nu\right)_{\alpha 1}\right|^2\right)^2 \frac{M_1^2\left(M_1^4 + M_\eta^4\right)}{\left(M_1^2 + M_\eta^2\right)^4} v_{\rm rel}^2, \tag{3.4}$$

$$\sigma^t_{\rm eff} v_{\rm rel} \simeq \frac{3\left(y_S\right)_{11}^2 y_t^2 M_1^2}{64\pi}\left|\frac{\sin\alpha\cos\alpha}{4M_1^2 - m_h^2 + i m_h \Gamma_h} - \frac{\sin\alpha\cos\alpha}{4M_1^2 - m_H^2 + i m_H \Gamma_H}\right|^2 \left(1 - \frac{m_t^2}{M_1^2}\right)^{3/2} v_{\rm rel}^2, \tag{3.5}$$

$$\sigma^h_{\rm eff} v_{\rm rel} \simeq \frac{\left(y_S\right)_{11}^4 \sin^4\alpha M_1^2}{32\pi\left(m_h^2 - 2M_1^2\right)^2}\left[1 - \frac{1}{3}\frac{m_h^2 - M_1^2}{m_h^2 - 2M_1^2} + \frac{1}{12}\left(\frac{m_h^2 - M_1^2}{m_h^2 - 2M_1^2}\right)^2\right]\sqrt{1 - \frac{m_h^2}{M_1^2}}\, v_{\rm rel}^2 \tag{3.6}$$

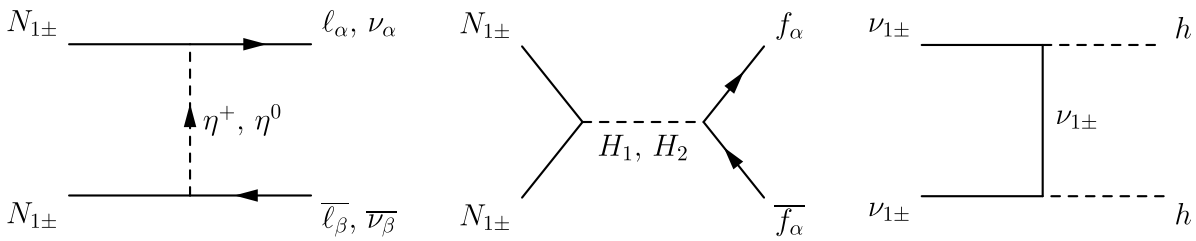

Figure 3: t, u and s-channel of coannihilation processes of DM $\nu_{1\pm}$.

where η_R, η_I and η^+ masses are regarded as same parameter M_η for simplicity and only top pair is taken into account in fermion pair $f\overline{f}$ because of the largeness of the Yukawa coupling. The SM-like Higgs mass and decay width are fixed to $m_h = 125$ GeV and $\Gamma_h = 10^{-2}$ GeV, and the heavy Higgs mass is assumed to be $m_H < 200$ GeV. The decay width of the heavy Higgs Γ_H is expressed as

$$\Gamma_H = \frac{y_t^2 \sin^2\alpha}{16\pi} m_H \left(1 - \frac{4m_t^2}{m_H^2}\right)^{3/2} . \tag{3.7}$$

The contribution of the process $H \to \nu_{1\pm}\nu_{1\pm}$ is also added to the decay width when the relation $m_H > 2M_1$ is satisfied. Note that the mixing matrix of charged leptons U_{eL} is introduced in the effective cross section $\sigma^\ell_{\rm eff} v_{\rm rel}$ since the initial Lagrangian (2.1) is not assumed as diagonal base of charged leptons. The s-wave vanishes and p-wave only remains in the above annihilation cross section due to the helicity suppression.

Since the neutrino Yukawa couplings y_ν are severely restricted by LFV, the annihilation cross section of $\ell\overline{\ell}$-channel is too small to obtain the proper DM relic abundance. Thus large contributions from $t\bar{t}$ and hh channels are required to have sizable effective annihilation cross section. These processes are possible because of the mixing of Higgses ϕ^0 and χ^0, namely the DMs $\nu_{1\pm}$ can be Higgs portal DMs. This is a different aspect from the loop induced neutrino mass model [6] and the various analysis of the right-handed neutrino DM in the original model [9, 39–42].

The independent parameters which appear in the analysis are Λ_1, Λ_3, M_1, M_3, M_η, m_H, $(y_S)_{11}$ and $\sin\alpha$. The parameters A and B of the neutrino mass matrix Eq. (2.11) are determined by neutrino mass eigenvalues as Eq. (2.14), and we take the fourth solution of Eq. (2.14) as example. The parameter λ of the charged lepton mixing matrix is fixed by the experimental value of $\sin\theta_{13}$ as Eq. (2.18), and Λ_2 and M_2 are not relative with the analysis since the second column of the neutrino Yukawa matrix Eq. (2.15) is zero. The allowed parameter spaces from LFV and the DM relic abundance for $(y_S)_{11} = 0.5$ and 1.0 in M_1-m_H plane are shown in Fig. 4 where the parameters are fixed to $\Lambda_i = 1$ eV, $M_2 = 1.5$ TeV and $M_3 = 2.0$ TeV. The parameter choice $\Lambda_i \sim 1$ eV means

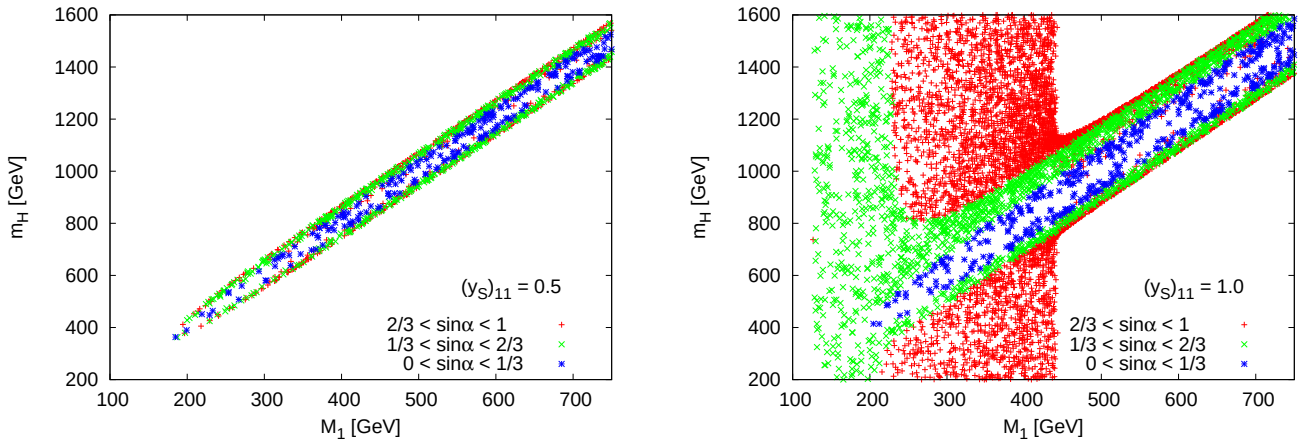

Figure 4: The allowed parameter spaces for $(y_S)_{11} = 0.5$ and 1.0 in M_1-m_H plane. The other parameters are fixed to $\Lambda_i = 1.0$ eV, $M_2 = 1.5$ TeV, $M_3 = 2.0$ TeV. The unfixed parameters are M_1, M_η, m_H and $\sin\alpha$.

that $\mu_i \sim 1$ keV if $I\left(M_i^2/m_R^2\right) \simeq I\left(M_i^2/m_I^2\right) \sim 0.1$ is assumed as can be seen from Eq. (2.10). The result does not practically depend on Λ_i, M_2 and M_3 since the dependence of Λ_i appears in only $\sigma_{\rm eff}^{\ell} v_{\rm rel}$ which has small annihilation cross section. Thus we can see that the appropriate contribution comes from the $t\bar{t}$-channel and hh-channel. The red, green and blue points correspond to each range of $\sin\alpha$ as written in Fig. 4. In the case of $(y_S)_{11} = 0.5$, the mass relation $2M_1 \approx m_H$ is required since the coupling $(y_S)_{11}$ is not so large and the annihilation cross section $\sigma_{\rm eff}^{t} v_{\rm rel}$ has to be enhanced due to a resonance. The resonance relation is not required for the right side one which corresponds to $(y_S)_{11} = 1.0$ if $\sin\alpha$ is large since the hh-channel is effective in this case. There is no allowed parameter space in $M_1 < m_h$ region because the main channel is $\nu_{1\pm}\nu_{1\pm} \to b\bar{b}$ and the contribution to the annihilation cross section is too small.

4 Direct Detection

The DM candidates $\nu_{1\pm}$ interact with quarks via Higgs exchange. Thus it is possible to explore the DM in direct detection experiments like XENON100 [33]. The Spin Independent (SI) elastic cross section $\sigma_{\rm SI}$ with nucleon N is given by

$$\sigma_{\rm SI}^N \simeq \frac{\mu_{\rm DM}^2}{\pi}\left(\frac{1}{m_h^2} - \frac{1}{m_H^2}\right)^2 \left(\frac{(y_S)_{11}\, m_N \sin\alpha\cos\alpha}{\sqrt{2}v}\sum_q f_q^N\right)^2, \tag{4.1}$$

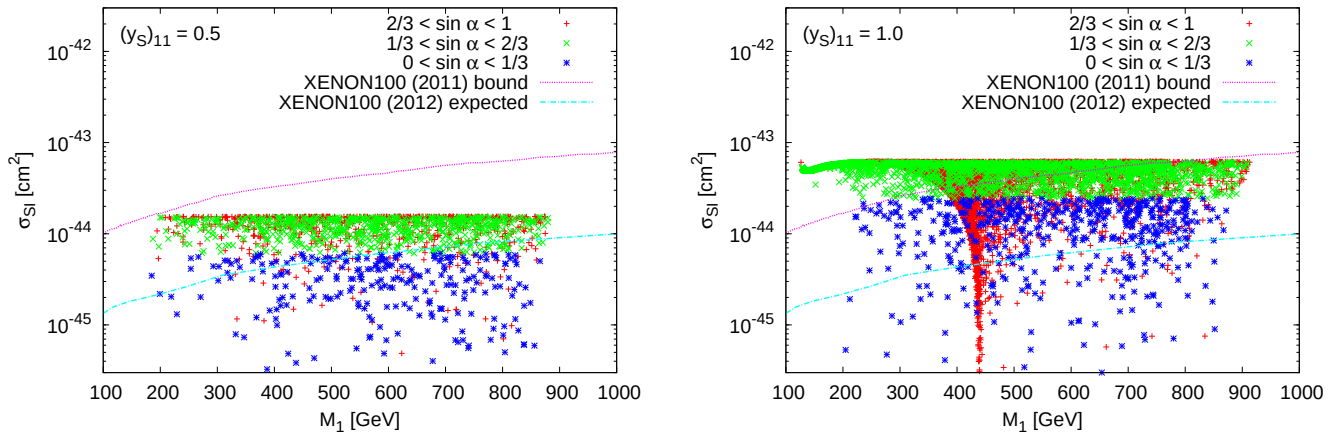

Figure 5: The comparison with XENON100 experiment. The left figure is for $(y_S)_{11} = 0.5$ and the right one is for $(y_S)_{11} = 1.0$. The parameter choice is same as Fig. 4.

where $\mu_{\rm DM} = \left(M_1^{-1} + m_N^{-1}\right)^{-1}$ is the DM-nucleon reduced mass and the heavy Higgs contribution is neglected. The parameters f_q^N which imply the contribution of each quark to nucleon mass are calculated by the lattice simulation [43, 44] as

$$f_u^p = 0.023, \quad f_d^p = 0.032, \quad f_s^p = 0.020, \tag{4.2}$$

$$f_u^n = 0.017, \quad f_d^n = 0.041, \quad f_s^n = 0.020, \tag{4.3}$$

for the light quarks and $f_Q^N = 2/27\left(1 - \sum_{q\leq 3} f_q^N\right)$ for the heavy quarks Q where $q \leq 3$ implies the summation of the light quarks. The recent another calculation is performed in Ref. [45].

The comparison with XENON100 upper bound is shown in Fig. 5 where the other parameters are fixed as same as Fig. 4 and these correspond to red, green and blue points. The violet dotted line is XENON100 (2011) upper bound and the light blue dashed line is XENON100 expected one in 2012. We can see that from the figure, the XENON100 (2011) limit excludes $M_1 \lesssim 800$ GeV in the large $\sin\alpha$ region for $(y_S)_{11} = 1.0$. The almost excluded region of rather small M_1 implies that the parameter region of the hh-channel is the most effective for the DM annihilation (Fig. 4). The other certain region will be verified by the future XENON experiment. In the case of taking into account the lightest right-handed neutrino as DM in the original radiative neutrino mass model [6], the elastic cross section with nuclei is not obtained at tree level because of the leptophilic feature of the DM. However interactions with quarks via Higgses are obtained in the radiative inverse seesaw model and hence verification by direct detection of DM is possible.

5 Conclusions

We constructed a radiative inverse seesaw model which generates neutrino masses and includes DMs simultaneously, and studied the mixing of the lepton sector and the DM features. The neutrino mass matrix was radiatively generated via the inverse seesaw framework. Considering the latest data of non-zero θ_{13}, we applied the charged lepton mixing effect with almost Maximal Dirac CP phase suggested by S. King. We can obtain the neutrino Dirac Yukawa matrix which produces the best fit value of θ_{12} on the diagonal basis of the right-handed neutrinos and additional fermions and non-zero θ_{13} comes from the charged lepton mixing matrix. The size of the neutrino Yukawa couplings is severely constrained by LFV at the same time. As a result, the annihilation cross section which comes from the Yukawa interaction becomes ineffective, however we found that new interactions via Higgs bosons which are independent on LFV. Thus the DM can have the certain annihilation cross section due to the interactions with Higgses. Verification of the model is also possible by direct detection of DM through the interaction with Higgses. In particular, the region of the large mixing $\sin\alpha$ will be testable by the exposure of the XENON100 (2012) experiment. Therefore it is favored to be Higgs portal DM in the radiative inverse seesaw model from the view point of avoiding the LFV constraint and obtaining the proper detection rate by direct search of DM.

Acknowledgments

H.O. thanks to Prof. Eung-Jin Chun, Dr. Priyotosh Bandyopadhyay, and Dr. Jong-Chul Park, for fruitful discussion. T. T. is supported by Young Researcher Overseas Visits Program for Vitalizing Brain Circulation Japanese in JSPS.

References

[1] R. N. Mohapatra, Phys. Rev. Lett. **56**, 561 (1986).

[2] R. N. Mohapatra and J. W. F. Valle, Phys. Rev. D **34**, 1642 (1986).

[3] W. Abdallah, A. Awad, S. Khalil and H. Okada, arXiv:1105.1047 [hep-ph].

[4] S. Khalil, Phys. Rev. D **82**, 077702 (2010) [arXiv:1004.0013 [hep-ph]].

[5] S. Khalil, H. Okada and T. Toma, JHEP **1107**, 026 (2011) [arXiv:1102.4249 [hep-ph]].

[6] E. Ma, Phys. Rev. D **73**, 077301 (2006) [arXiv:hep-ph/0601225].

[7] L. M. Krauss, S. Nasri and M. Trodden, Phys. Rev. D **67**, 085002 (2003) [arXiv:hep-ph/0210389].

[8] M. Aoki, S. Kanemura and O. Seto, Phys. Rev. Lett. **102**, 051805 (2009) [arXiv:0807.0361].

[9] D. Schmidt, T. Schwetz and T. Toma, Phys. Rev. D **85**, 073009 (2012) [arXiv:1201.0906 [hep-ph]].

[10] R. Bouchand and A. Merle, arXiv:1205.0008 [hep-ph].

[11] E. Ma, A. Natale and A. Rashed, arXiv:1206.1570 [hep-ph].

[12] M. Aoki, J. Kubo, T. Okawa and H. Takano, Phys. Lett. B **707**, 107 (2012) [arXiv:1110.5403 [hep-ph]].

[13] Y. H. Ahn and H. Okada, Phys. Rev. D **85**, 073010 (2012) [arXiv:1201.4436 [hep-ph]].

[14] Y. Farzan and E. Ma, arXiv:1204.4890 [hep-ph].

[15] F. Bonnet, M. Hirsch, T. Ota and W. Winter, arXiv:1204.5862 [hep-ph].

[16] K. Kumericki, I. Picek and B. Radovcic, arXiv:1204.6597 [hep-ph].

[17] K. Kumericki, I. Picek and B. Radovcic, arXiv:1204.6599 [hep-ph].

[18] E. Ma, arXiv:1206.1812 [hep-ph].

[19] G. Gil, P. Chankowski and M. Krawczyk, arXiv:1207.0084 [hep-ph].

[20] M. Aoki, S. Kanemura, T. Shindou and K. Yagyu, JHEP **1007**, 084 (2010) [Erratum-ibid. **1011**, 049 (2010)] [arXiv:1005.5159 [hep-ph]].

[21] S. Kanemura, O. Seto and T. Shimomura, Phys. Rev. D **84**, 016004 (2011) [arXiv:1101.5713 [hep-ph]].

[22] M. Lindner, D. Schmidt and T. Schwetz, Phys. Lett. B **705**, 324 (2011) [arXiv:1105.4626 [hep-ph]].

[23] S. Kanemura, T. Nabeshima and H. Sugiyama, Phys. Rev. D **85**, 033004 (2012) [arXiv:1111.0599 [hep-ph]].

[24] Z. Maki, M. Nakagawa and S. Sakata, Prog. Theor. Phys. **28**, 870 (1962).

[25] M. Tortola, J. W. F. Valle and D. Vanegas, arXiv:1205.4018 [hep-ph].

[26] T2K Collaboration: K. Abe *et al.*, Phys. Rev. Lett. **107**, 041801 (2011).

[27] Y. Abe *et al.* [DOUBLE-CHOOZ Collaboration], Phys. Rev. Lett. **108**, 131801 (2012) [arXiv:1112.6353 [hep-ex]].

[28] Daya Bay Collaboration: F. P. An *et al.*, arXiv:1203.1669 [hep-ex].

[29] RENO Collaboration: J. K. Ahn *et al.*, arXiv:1204.0626 [hep-ex].

[30] S. Antusch and S. F. King, Phys. Lett. B **631**, 42 (2005) [hep-ph/0508044];

[31] S. F. King, arXiv:1205.0506 [hep-ph].

[32] E. Komatsu *et al.* [WMAP Collaboration], Astrophys. J. Suppl. **192**, 18 (2011) [arXiv:1001.4538 [astro-ph.CO]].

[33] E. Aprile *et al.* [XENON100 Collaboration], Phys. Rev. Lett. **107**, 131302 (2011) [arXiv:1104.2549 [astro-ph.CO]].

[34] E. Ma, Phys. Rev. D **80**, 013013 (2009) [arXiv:0904.4450 [hep-ph]].

[35] M. S. Carena, A. Daleo, B. A. Dobrescu and T. M. P. Tait, Phys. Rev. D **70**, 093009 (2004) [hep-ph/0408098].

[36] W. Rodejohann, Int. J. Mod. Phys. E **20**, 1833 (2011) [arXiv:1106.1334 [hep-ph]].

[37] J. Adam *et al.* [MEG Collaboration], Phys. Rev. Lett. **107**, 171801 (2011) [arXiv:1107.5547 [hep-ex]].

[38] K. Nakamura *et al.* [Particle Data Group Collaboration], J. Phys. G G **37**, 075021 (2010).

[39] J. Kubo, E. Ma and D. Suematsu, Phys. Lett. B **642**, 18 (2006) [hep-ph/0604114].

[40] J. Kubo and D. Suematsu, Phys. Lett. B **643**, 336 (2006) [hep-ph/0610006].

[41] D. Suematsu, T. Toma and T. Yoshida, Phys. Rev. D **79**, 093004 (2009) [arXiv:0903.0287 [hep-ph]].

[42] D. Suematsu and T. Toma, Nucl. Phys. B **847**, 567 (2011) [arXiv:1011.2839 [hep-ph]].

[43] A. Corsetti and P. Nath, Phys. Rev. D **64**, 125010 (2001) [hep-ph/0003186].

[44] H. Ohki, H. Fukaya, S. Hashimoto, T. Kaneko, H. Matsufuru, J. Noaki, T. Onogi and E. Shintani *et al.*, Phys. Rev. D **78**, 054502 (2008) [arXiv:0806.4744 [hep-lat]].

[45] J. M. Alarcon, J. Martin Camalich and J. A. Oller, Phys. Rev. D **85**, 051503 (2012) [arXiv:1110.3797 [hep-ph]].